Journal of Quantitative Spectroscopy & Radiative Transfer 276 (2021) 107911

Contents lists available at ScienceDirect

Journal of Quantitative Spectroscopy & Radiative Transfer

journal homepage: www.elsevier.com/locate/jqsrt

Accurate calculations of beyond-Voigt line-shape parameters from first principles for the He-perturbed HD rovibrational lines: A comprehensive dataset in the HITRAN DPL format

Kamil Stankiewicz[a,*], Nikodem Stolarczyk[a], Hubert Jóźwiak[a], Franck Thibault[b], Piotr Wcisło[a]

[a] Institute of Physics, Faculty of Physics, Astronomy and Informatics, Nicolaus Copernicus University, Grudziądzka 5, Toruń, 87–100, Poland
[b] Univ Rennes, CNRS, IPR (Institut de Physique de Rennes)-UMR 6251, F-35000 Rennes, France

ARTICLE INFO

Article history:
Received 12 July 2021
Revised 26 August 2021
Accepted 27 August 2021
Available online 28 August 2021

Keywords:
HD
He
HITRAN
Line–shape parameters
Beyond-Voigt
Quantum scattering

ABSTRACT

We report a comprehensive dataset of beyond-Voigt line-shape parameters (pressure broadening and shift coefficients, their speed-dependences, and the complex Dicke parameters) for all electric dipole and quadrupole transitions within the ground electronic state in He-perturbed HD that are present in the HITRAN database. The parameters are determined from generalized spectroscopic cross-sections which we obtain by solving *ab initio* quantum scattering problem using the close-coupling formulation and the state-of-the-art potential energy surface of the HD-He interaction. We parametrize the temperature dependence of the line-shape parameters with double-power-law representation (DPL), recommended for the HITRAN database. Comparison with the analogous results for the H_2-He system reveals a strong isotopologue dependence.

1. Introduction

Due to its abundance in the Universe, molecular hydrogen is an object of interest in various fields. Because of its simplicity, it is a benchmark system for testing *ab initio* quantum chemistry calculations [1,2] and quantum electrodynamics for molecules [3,4]. Despite its small natural abundance, the HD isotopologue is notable in spectroscopy of gas giants' atmospheres due to the presence of permanent dipole moment, and thus, dipole transitions, the intensities of which are much larger than those of weak quadrupole lines in H_2. HD also possesses a smaller rotational constant than H_2 which entails smaller rotational spacing of the energy levels. Those two facts result in the potential domination of HD molecules in the process of primordial gas cooling under specific physical conditions [5]. The D/H ratios, which are mainly obtained from measurement of abundances of H_2 and HD, are also essential indicators of planetary formation and evolution [6,7]. For precise measurements, a list of accurate values of line-shape parameters is crucial [6,8]. For some observations [6], it turns out that the errors in the analysis can be dominated by the uncertainties of self- and helium-perturbed line-shape parameters.

A mixture of molecular hydrogen and atomic helium is the main constituent of the atmospheres of gas giants in the Solar System. It is also predicted to be a dominant component of atmospheres of some types of exoplanets [9]. Thus, the relevant collisional systems, for which line-shape parameters are sought after, are: H_2 - H_2, H_2-He, HD-H_2, and HD-He. The importance of the beyond-Voigt line-shape parameters was widely discussed in previous studies [10–18]. Populating the entire database of the line-shape parameters for a large number of transitions and different thermodynamical conditions with experimentally determined values is a very challenging task. Not only is it hard because of the wide spectral range of transitions and different measurements' conditions but also due to strong numerical correlations between the line-shape parameters [19]. This problem was addressed by the implementation of a method that allows obtaining accurate line-shape parameters through *ab initio* quantum scattering calculations. The method has been already used for thorough examination of the H_2-He system [1,20,21], which resulted in the first comprehensive dataset of beyond-Voigt line-shape parameters [19] which covers all electric rovibrational transitions within the ground electronic level that are present in the HITRAN

* Corresponding author.
E-mail addresses: stankiewiczkamil98@gmail.com (K. Stankiewicz), piotr.wcislo@umk.pl (P. Wcisło).

https://doi.org/10.1016/j.jqsrt.2021.107911

database [22] for a wide range of temperatures. The results of those *ab initio* calculations were successfully experimentally verified for several lines [19,23,24]. In the case of the HD-He system, the line-shape parameters for several rotational lines were investigated theoretically and experimentally [25] and calculations for several dozens of dipole rovibrational transitions were conducted [26].

In this work, we utilize the method of obtaining the collisional line-shape parameters through *ab initio* quantum scattering calculations that was presented in Ref. [19], to populate all electric dipole and quadrupole transitions within the ground electronic state that are present in the HITRAN database for He-perturbed HD. Using the state-of-the-art potential energy surface obtained through quantum chemical calculations [1,2] we solve the quantum scattering problem by adopting the close-coupling formulation and obtain the scattering matrices. They are used to calculate the generalized spectroscopic cross-sections (GSXS) which are utilized to derive line-shape parameters that describe pressure broadening, shift, their speed-dependences, and the effect of the velocity-changing collisions. Temperature dependences of the line-shape parameters are expressed using the double-power-law (DPL) representation, which is the recommended parametrization for the HITRAN database [27]. Section 2 provides the details of the calculations. In Section 3, we discuss the dependences of the GSXS and line-shape parameters on the vibrational band, initial rotational level, and the performance of the DPL parametrization. For completeness, we interpolate and extrapolate our large set of *ab initio* calculated line-shape parameters to populate all electric dipole and quadrupole rovibrational transitions within the ground electronic state that are present in the HITRAN database. We also compare our results with the ones presented in Ref. [19] for the H_2-He system. We observe a strong isotopologue dependence which is in contradiction to the results measured for more massive molecules. The GSXS and *ab initio* values of line-shape parameters for calculated lines, as well as DPL coefficients, are provided in the supplementary material [28].

2. Calculations

This section presents the methodology used to obtain the line-shape parameters from *ab initio* calculations for a collisional system consisting of a diatomic molecule and a structureless atom. Section 2.1 describes how to determine the line-shape parameters from the GSXS and Section 2.2 briefly explains the process of obtaining GSXS through quantum scattering calculations.

2.1. Line shape parameters

The pressure broadening and shift of the spectral line may be described by the pressure broadening $\gamma(v)$ and pressure shift $\delta(v)$ coefficients which are functions of the speed, v, of the active molecule (the coefficients also depend on the temperature but for short we do not write it explicitly). They may be obtained from first principles by calculating the generalized spectroscopic cross-section, σ_0^q, (which is described in the next subsection) and averaging it over the velocity distribution of relative motion of the active molecule and the perturber [29–31]:

$$\gamma(v)+\mathrm{i}\delta(v)=\frac{1}{2\pi c}\frac{1}{k_BT}\frac{2}{\sqrt{\pi}\bar{v}_p v}\times \int_0^\infty v_r^2\exp\left(-\frac{v^2+v_r^2}{\bar{v}_p^2}\right)\sinh\left(\frac{2vv_r}{\bar{v}_p^2}\right)\sigma_0^q(v_r)dv_r, \tag{1}$$

where v_r is the relative speed of colliding partners, $\bar{v}_p$ is the most probable speed of the perturber, k_B is the Boltzmann constant, c is the speed of light, and T denotes temperature.

For most applications, it is inconvenient to store the full speed-dependence of $\gamma(v)$ and $\delta(v)$ and use it in the data analysis. For this reason the new HITRAN DPL format [19,27] adopts their quadratic approximation [32,33]:

$$\gamma(v)+i\delta(v)\approx\gamma_0+i\delta_0+(\gamma_2+i\delta_2)\left(\frac{v^2}{v_m^2}-\frac{3}{2}\right), \tag{2}$$

where v_m denotes the most probable speed of the absorber. γ_0 and δ_0 are the speed-averaged pressure broadening and shift coefficients, which can be calculated directly from [11,27]:

$$\gamma_0+\mathrm{i}\delta_0=\frac{1}{2\pi c}\frac{1}{k_BT}\langle v_r\rangle\int_0^\infty xe^{-x}\sigma_0^q(xk_BT)dx, \tag{3}$$

where $x=E_{kin}/k_BT$, E_{kin} is the relative kinetic energy of the collision partners and $\langle v_r\rangle$ is the mean value of their relative speed. Alternatively, γ_0 and δ_0 may be obtained by averaging Eq. (2) over the Maxwell-Boltzmann distribution of the absolute speed at given temperature, T. Parameters γ_2 and δ_2 are obtained by imposing the condition that the slopes of the actual speed-dependence and the quadratic approximation are equal at the most probable absorber speed, v_m:

$$\frac{2}{v_m}(\gamma_2+i\delta_2)=\frac{d}{dv}(\gamma(v)+i\delta(v))|_{v=v_m}. \tag{4}$$

Using this condition together with Eqs. (1) and (2) one can write explicit formula for γ_2 and δ_2 [19]:

$$\gamma_2+i\delta_2=\frac{1}{2\pi c}\frac{1}{k_BT}\frac{\bar{v}_p}{\sqrt{\pi}}e^{-y^2}\times \int_0^\infty\left(2z\cosh(2zy)-\left(\frac{1}{y}+2y\right)\sinh(2zy)\right)\times z^2e^{-z^2}\sigma_0^q(z\bar{v}_p)dz, \tag{5}$$

where y denotes the $v_m/\bar{v}_p$ ratio and z is equal to $v_r/\bar{v}_p$.

The impact of velocity-changing collisions is quantified by the complex Dicke parameter $\tilde{\nu}_{opt}$, which is also known as the optical frequency of the velocity-changing collisions. It can be calculated as:

$$\tilde{\nu}_{opt}=\tilde{\nu}_{opt}^r+i\tilde{\nu}_{opt}^i=\frac{1}{2\pi c}\frac{1}{k_BT}\langle v_r\rangle M_a\times \int_0^\infty xe^{-x}\left[\frac{2}{3}x\sigma_1^q(xk_BT)-\sigma_0^q(xk_BT)\right]dx, \tag{6}$$

where $M_a=\frac{m_p}{m_a+m_p}$, m_a and m_p are the masses of the active molecule and the perturber and σ_1^q is the Dicke cross-section.

Altogether, we report six collisional line-shape parameters: γ_0, δ_0, γ_2, δ_2, $\tilde{\nu}_{opt}^r$ $\tilde{\nu}_{opt}^i$, and we provide their temperature dependences using the double-power-law (DPL) [27] format, recommended for the HITRAN database [22]:

$$\begin{aligned}
\gamma_0(T)&=g_0(T_{ref}/T)^n+g_0'(T_{ref}/T)^{n'},\\
\delta_0(T)&=d_0(T_{ref}/T)^m+d_0'(T_{ref}/T)^{m'},\\
\gamma_2(T)&=g_2(T_{ref}/T)^j+g_2'(T_{ref}/T)^{j'},\\
\delta_2(T)&=d_2(T_{ref}/T)^k+d_2'(T_{ref}/T)^{k'},\\
\tilde{\nu}_{opt}^r(T)&=r(T_{ref}/T)^p+r'(T_{ref}/T)^{p'},\\
\tilde{\nu}_{opt}^i(T)&=i(T_{ref}/T)^q+i'(T_{ref}/T)^{q'},
\end{aligned} \tag{7}$$

for $T_{ref}=296$ K. The *ab initio* values of the line-shape parameters are calculated at different temperatures ranging from 20 to 1000 K and then projected on the DPL representation. Due to its importance from the perspective of the gas giants' atmospheric observations, we prioritized the temperature range between 50 and 200 K by applying weights magnified tenfold in the fitting procedure.

2.2. Generalized spectroscopic cross-sections

In order to obtain the GSXS, one needs to solve the Schrödinger equation for the atom-molecule scattering problem and find the

scattering matrices describing the completed collision process. The problem may be addressed through the close-coupling formulation [34,35]. In the case of collision between a diatom molecule and a structureless atom, the potential energy surface (PES), $V(R, r, \theta)$, depends only on three variables – R, which is the distance between the atom and the center of mass of the molecule, r, which is the internal distance between the nuclei in the molecule, and θ, which is the angle between the molecular axis and the axis connecting the atom with the center of mass of the molecule. In our calculations, we use the current state-of-the-art BSP3 PES [1] which is an upgraded version of the Bakr, Smith, Patkowski PES [2]. Because this PES is calculated within the Born-Oppenheimer approximation, it may be used to describe the HD-He interaction by simply shifting the center of mass of the molecule. The dependence on θ is separated by expanding the potential in terms of Legendre polynomials:

$$V(R, r, \theta) = \sum_{\xi=0}^{\xi_{max}} v_{\xi}(R, r) P_{\xi}(\cos\theta). \tag{8}$$

In our calculation, we truncate the expansion at $\xi_{\max} = 6$ which gives accurate results due to the small anisotropy of the system [25]. The PES is further expanded in terms of radial molecular wavefunctions $\chi_{v,j}(r)$ of the HD molecule to separate the dependence on r and obtain the radial coupling potential terms:

$$A_{\xi,v,j,v',j'}(R) = \int_0^{\infty} \chi_{v',j'}(r) v_{\xi}(R, r) \chi_{v,j}(r) dr, \tag{9}$$

We neglect any vibrational coupling, thus for all non-zero radial terms $v = v'$. Usually, for rovibrational transitions, the centrifugal distortion coming from the difference in the shape of radial molecular wavefunctions for different j is neglected [20] which results in the assumption that $j = j' = 0$. However, it was shown recently [26] that in the case of such a light molecule as HD, the centrifugal distortion cannot be disregarded if one seeks a sub-percent accuracy, especially for transitions that include higher rotational levels.

The quantum scattering calculations are performed using the BIGOS code [36] for kinetic energies (E_{kin}) ranging from 0.1 cm^{-1} to 9000 cm^{-1}. Propagation is carried out between 0.1 and 200 a_0 using the renormalized Numerov's algorithm [37] and log-derivative method [38]. Based on calculations for one transition, we determine the value of numerical parameters – propagator's step and the number of closed channels (i.e rovibrational levels in the basis, the energy of which is higher than the total energy of the system) such that they provide sub-percent accuracy for the relevant range of E_{kin}. The determined step of the propagator depends on the energy of the collision, and the number of closed channels is set to 3 (see Section 4 from Ref. [26]). Using boundary conditions imposed on the wavefunction of the system one can obtain the scattering matrix [39] and use it to calculate the GSXS [40,41]:

$$\begin{aligned}\sigma_{\lambda}^{q}(v_i, j_i, v_f, j_f; E_{kin}) = {} & \tfrac{\pi}{k^2} \textstyle\sum_{J_i J_f, l, l', \bar{l}, \bar{l}'} \mathrm{i}^{l-l'-\bar{l}+\bar{l}'} \\ & \times (-1)^{l-l'-\bar{l}+\bar{l}'} [J_i][J_f] \sqrt{[l][l'][\bar{l}][\bar{l}']} \begin{pmatrix} l & \bar{l} & \lambda \\ 0 & 0 & 0 \end{pmatrix} \\ & \times \begin{pmatrix} l' & \bar{l}' & \lambda \\ 0 & 0 & 0 \end{pmatrix} \begin{bmatrix} j_i & j_i & \bar{l} & \bar{l}' \\ j_f & l & j_f & l' \\ q & J_f & J_i & \lambda \end{bmatrix} [\delta_{ll'} \delta_{\bar{l}\bar{l}'} \\ & - \langle v_i j_i l' | \mathbf{S}^{J_i}(E_{T_i}) | v_i j_i l \rangle \langle v_f j_f \bar{l}' | \mathbf{S}^{J_f}(E_{T_f}) | v_f j_f \bar{l} \rangle^*]. \end{aligned} \tag{10}$$

In the equation above v_i, j_i, v_f, j_f denote the initial and final states of the optical transition. J_i and J_f are the total angular momenta associated with the initial and final spectroscopic levels, E_{T_i}, E_{T_f} are the total energies of the system in the initial and final spectroscopic states, k is the wavenumber corresponding to the initial kinetic energy, l is the relative angular momentum and E_{kin} is the relative kinetic energy which is the same in both initial and final states of transition. The symbol $[x]$ stands for $(2x + 1)$, the matrix written in square brackets is the Wigner 12-j symbol of the second kind, the matrices in the parenthesis are Wigner 3-j symbols, and q denotes the rank of the radiation-matter interaction tensor. For quadrupole lines $q = 2$ and for dipole lines $q = 1$. The real and imaginary parts of σ_0^q are the pressure broadening and pressure shift cross-sections (PBXS and PSXS, respectively) [42–44] while σ_1^q is the complex Dicke cross-section [40,44,45], the real and imaginary parts of which are denoted by RDXS and IDXS, respectively.

3. Results

The full procedure described in the previous section is conducted for all electric dipole and quadrupole transitions within the ground electronic state for which both the initial and final levels of the HD molecule are described by vibrational levels 0 to 5 and 8, and rotational levels from 0 to 6 and 9 to 11, including hot bands. Such a wide range of vibrational and rotational states allows us to obtain results containing all the most important and the strongest transitions as well as a great number of weaker ones. For each of these transitions, we obtain the GSXS at E_{kin} of HD-He relative motion ranging from 0.1 to 9000 cm^{-1}. The GSXS are used to obtain the line-shape parameters as described in Section 2.1. The temperature dependence of the latter is projected onto the DPL structure [19,27]. The GSXS, the values of line-shape parameters, and the DPL coefficients are provided in the supplementary materials [28]. This work extends the *ab initio* calculations reported in Ref. [26] by the inclusion of the quadrupole transitions, providing speed-dependence parameters, γ_2 and δ_2, performing some additional calculations for transitions involving higher j and v, and expressing the temperature dependence of line-shape parameters with convenient DPL parametrization for the database application. For completeness, to populate all lines within the ground electronic state that are present in the HITRAN database [22] with beyond-Voigt line-shape parameters, we extrapolate our *ab initio* results of the line-shape parameters obtained from calculated GSXS. We also compare our results with calculations for H_2-He system [19] and observe a strong isotopologue dependence between them.

3.1. Quantum scattering calculations

In this section, we present the results of our quantum scattering calculations for selected transitions. We also discuss the difference between GSXS for H_2-He and HD-He collisional systems on the example of several selected lines.

Fig. 1 shows examples of the GSXS for the cases of the O(2), Q(1), and S(0) lines for different vibrational bands, as a function of the relative kinetic energy of HD-He motion. In the case of dipole lines, a similar presentation was already published and discussed in Ref. [26]. In each panel, the GSXS are compared between vibrational bands from 1-0 to 5-0 and 8-0.

Both the PSXS and IDXS change their signs as the relative kinetic energy increases. The reason for this behavior in the case of the PSXS was presented in Ref. [21] and related to the fact that collisions occurring at different relative kinetic energies probe different regions of the PES. For each rovibrational transition in every branch, the change of the PSXS sign occurs at similar E_{kin} around 10 to 30 cm^{-1}. For the IDXS the change can be observed at E_{kin} around 150 to 300 cm^{-1}. Near the energy at which the PSXS changes its sign, the PBXS reaches its minimum.

It can be seen that the values of the PBXS, RDXS as well as the absolute values of the PSXS and IDXS increase with the vibrational band. For the RDXS, such behavior becomes noticeable

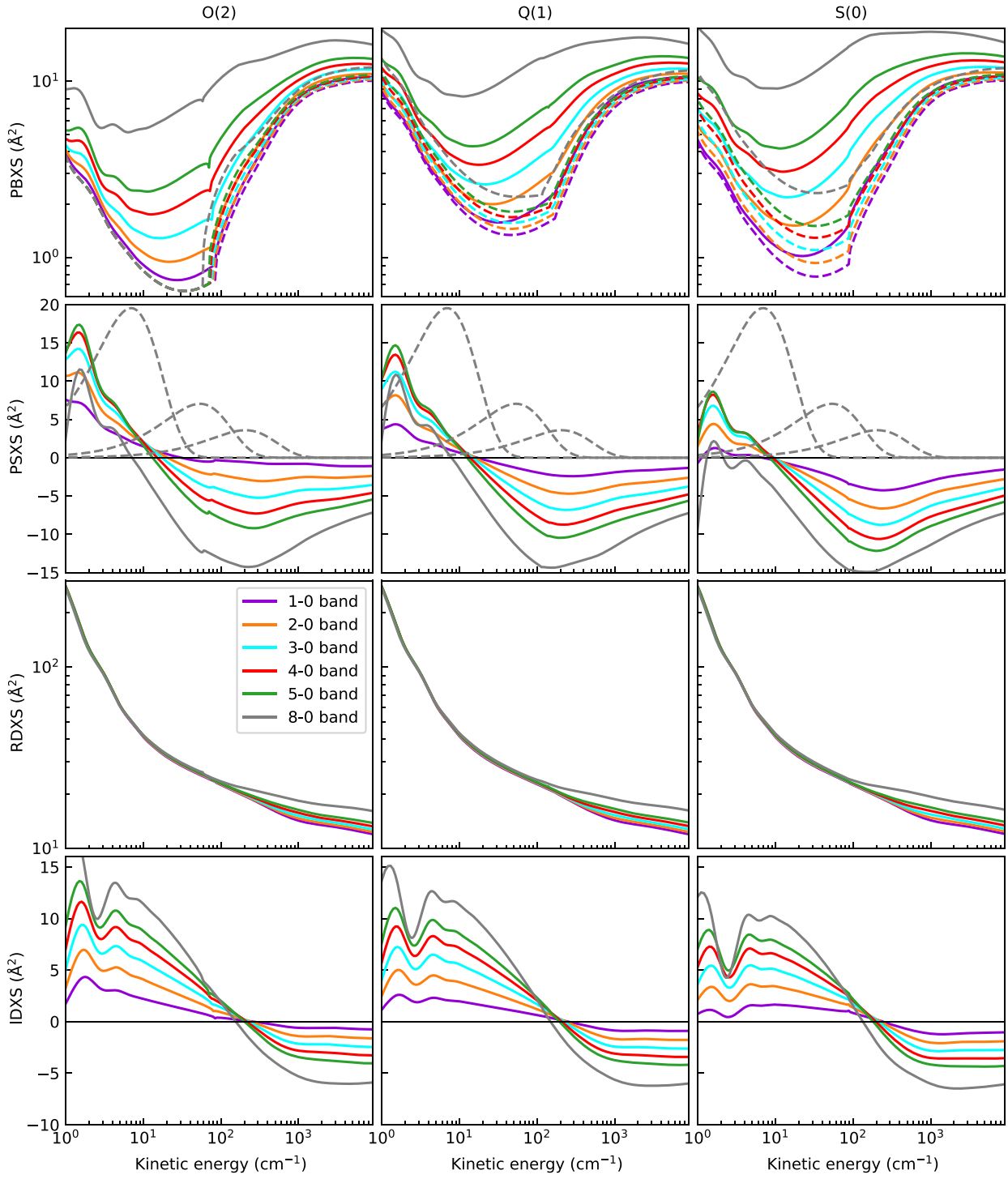

Fig. 1. The PBXS, PSXS, RDXS, and IDXS compared between vibrational bands as a function of the relative motion of HD and He for the O(2), Q(1), and S(0) lines. The inelastic contribution to the PBXS is represented by colored dashed lines in the upper panel. The dashed gray lines in the second row show the Maxwell-Boltzmann distributions at 10 K, 77 K, and 296 K.

at E_{kin} higher than around 200 cm^{-1}. In the case of the PSXS, such behavior is seen at K.E higher than around 10 cm^{-1}. This dependence on the vibrational band results from two phenomena. Firstly, a significant contribution to the PBXS and PSXS for rovibrational transitions comes from rovibrational dephasing. It mainly originates from the difference in the isotropic part of the PES in the initial and final molecular state, which increases with the difference between initial and final vibrational levels. Secondly, the rotational spacing of energy levels decreases with increasing vibrational state, which enlarges the inelastic contribution to the cross-section. It can be easily separated for the PBXS and is marked by colored dashed lines in Fig. 1.

One may notice that for some lines a sharp change of the GSXS can be observed at a certain E_{kin} This is caused by the opening of the first inelastic energy channel in the initial or final molecular state of the optical transition. The opening occurs when the ki-

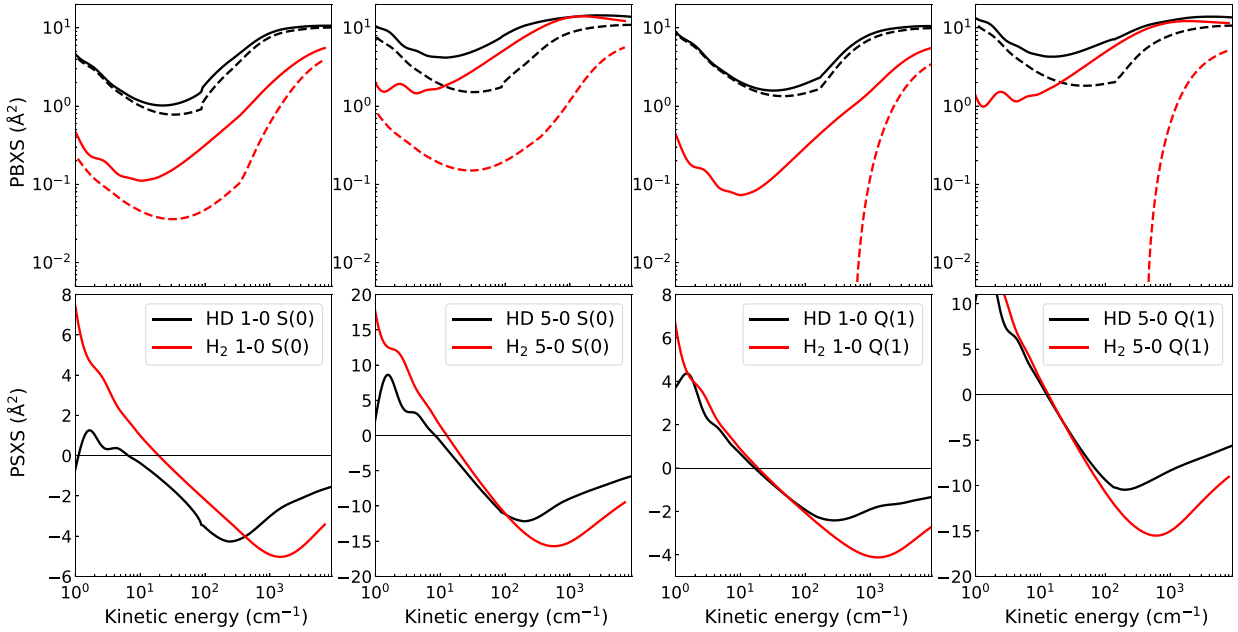

Fig. 2. Comparison of the PBXS and PSXS in HD-He and H_2-He collisional systems for several selected transitions. Starting from the left panels transitions 1-0 S(0), 5-0 S(0), 1-0 Q(1) and 5-0 Q(1) are shown. The dashed lines correspond to the inelastic contribution to the pressure broadening cross-section.

netic energy of the relative motion becomes high enough to induce collisional rotational excitation of the molecule. This may result in a rapid change of the inelastic part of the cross-section. The fact that the rotational constant decreases with the vibrational quantum number explains why the PBXS of O lines split at slightly different E_{kin} (see also Figure 1 and discussion about the $P_\nu(1)$ and $R_\nu(0)$ lines in Ref. [26]).

In Fig. 2, a comparison of the PBXS and PSXS between selected quadrupole lines in the HD-He and H_2-He collisional systems are presented. The values of the GSXS for the H_2-He system are taken from Ref. [19]. One can immediately notice that in the case of transitions belonging to the fundamental band, the PBXS for the H_2-He system is significantly smaller than in the case of the HD-He system. The difference comes mainly from the inelastic part of the PBXS, which is a dominant component of the cross-sections for the HD molecule and is significantly greater than the inelastic contribution in the case of H_2. This is further magnified at low K.E in the Q(1) line, where the inelastic contribution is exactly zero for the H_2 molecule. The elastic part generally exhibits a smaller difference between the two systems. The behavior of inelastic contribution is explained as follows. Firstly, the energy spacing between rotational levels is larger in the H_2 than in the HD isotopologue. Secondly, the collisions do not induce transitions between even and odd rotational levels for H_2, since they cannot change the nuclear spin of the molecule. In contrast, the leading anisotropic component of the HD-He PES, the $A_{\xi=1,\nu,j,\nu',j'}$ term, allows $\Delta j = |j_f - j_i| = 1$ transitions.

The situation is different for transitions between states for which the difference in vibrational level $\Delta\nu = \nu_f - \nu_i$ is large. In such cases, the dominance of the PBXS cross-section value of HD over H_2 is not that pronounced, because the elastic part of the PBXS starts to play a more important role, as the difference between initial and final molecular wavefunction becomes larger. This can be seen in the panels from the second and fourth columns in Fig. 2. Generally, the elastic part of the PBXS is larger for HD molecule at lower K.E range and smaller at higher E_{kin} This suggests a larger difference between the initial and final states in terms of the repulsive part of the PES of hydrogen-helium interaction as the high-energy collisions probe the repulsive short-range of the PES. For some transitions between states that differ significantly in terms of ν and j, in a certain E_{kin} range, the value of the PBXS in H_2-He system may become larger than in the HD-He system. Finally, the PSXS is similar for the two collisional systems.

3.2. Dataset of beyond-Voigt line-shape parameters

In this section, we describe the final result of our work, i.e., the comprehensive dataset of the beyond-Voigt spectral line-shape parameters of HD perturbed by He. Our dataset covers all the 11 575 rovibrational lines present in the HITRAN database, including electric dipole transitions from the P and R branches, as well as the O, Q, and S electric quadrupole lines. We perform the *ab initio* calculations described in Section 2 to obtain the line-shape parameters for the basic set of 875 transitions at temperatures spanning from 20 to 1000 K. Our calculations are based on the cross-sections which are provided in the supplementary materials to this work [28]. The data for the remaining 10 700 lines (the majority belong to the hot-band lines) comes from interpolation and extrapolation of the data from our basic set. Let us denote a given transition as X(j'') ν' - ν'', where X∈{O, Q, P, R, S} denotes the branch, j'' is the rotational quantum number of the initial state, and ν' and ν'' are the final and initial vibrational states, coupled by the transition. We also denote $\Delta\nu = \nu' - \nu''$. Using this notation, let us describe our interpolation and extrapolation scheme with the following steps (note that after each step the interpolated and extrapolated lines are appended to the basic set).

- if there are at least three lines with the same X, ν' and ν'' in our initial dataset, we use a second-order polynomial to interpolate the missing lines as a function of j'', up to the highest $j'' = j''_{\max}$ from our basic set. For $j'' > j''_{\max}$ we copy the dataset entries of X($j''_{\max}$) ν' - ν'' lines.
- If there are at least three lines with the same X, j'' and ν'', we use a second-order polynomial to interpolate the missing lines in the function of ν', up to the highest $\nu' = \nu'_{\max}$ from our basic

set. For $\nu' > \nu'_{max}$ we copy the dataset entries of X(j'') ν'_{max} - ν'' lines.
- For each X and j'' we select the lines with the lowest $\Delta\nu = \Delta\nu_{min}$ (i.e., 1-0, 2-1, 3-2... for the O, P and Q branches and 0-0, 1-1, 2-2... for the R and S branches). We extrapolate these subsets with a second-order polynomial in the function of ν'' to obtain entries for the high hot bands with $\Delta\nu = \Delta\nu_{min}$.
- For each X and j'' we approximate the missing hot band entries maintaining constant distances between different subsets with the same $\Delta\nu$, i.e., X(j'') $\nu' - \nu''$ = X(j'') $\Delta\nu$ - 0 - X(j'') $\Delta\nu_{min}$ - 0 + X(j'') ($\nu'' + \Delta\nu_{min}$) - ν'' (for example S(0) 4-2 = S(0) 2-0 - S(0) 0-0 + S(0) 2-2).

The above interpolation and extrapolation scheme is repeated for every considered temperature. We apply the DPL representation defined by Eqs. (7) to represent the temperature dependences in a form adopted in the HITRAN database [27] and recently applied for the H_2-He system [19]. We perform a weighted fitting procedure in the 20 – 1000 K temperature range, prioritizing the range between 50 and 200 K (see the gray-shaded areas in Fig. 3).

Fig. 3 presents examples of the DPL representation applied to the cases of two purely rotational lines, S(0) and R(0) from 0-0 band, and two rovibrational lines, Q(1) 1-0 and R(1) 1-0. The general performance of DPL is satisfying and comparable with the one presented in Ref. [27] on an example of a few collisional systems. As noticed in Refs. [19,27], DPL works the best when the temperature dependence of the line-shape parameters is monotonic, and its performance is worse when sharp extrema are present as can be seen in Fig. 3.

The highest discrepancy can be observed for the δ_2 parameter of the S(0) 0-0 line. However, as shown in Ref. [24] for H_2 isotopologue, the neglection of the speed-dependence effect, which for this molecule has an exceptionally high impact, introduces a change of the line-shape up to a level of a few percent. Thus, in the most important temperature region and its proximity, applying the DPL is expected to cause, at most, sub-percent change of the line-shape due to inaccuracy of δ_2 representation. Good performance of the DPL approximation in the case of the $\tilde{\nu}^r_{opt}$ may be related to the fact that it can be quite accurately determined from the diffusion coefficient which satisfies the power law temperature dependence [27]. Comparison with analogous results calculated for H_2-He collisional system [19] leads to the observation that both isotopologues H_2 and HD portray similar dependence of the line-shape parameters on temperature.

The dependences of the line-shape parameters on the vibrational band and initial rotational level of the transition are shown in Fig. 4. We present the parameters at two temperatures – 150 K and 296 K. For comparison, in the case of γ_0 and δ_0, we also include the data for the H_2-He collisional system at 296 K [19]. Contrarily to the results obtained for more massive species, such as self- or foreign-gas-perturbed CO, SO_2 and OCS [46–49], the difference between the results for H_2 and HD is pronounced. Therefore we question the "isotopic invariance" paradigm by demonstrating strong isotopologue dependence of the line-shape parameters.

The differences between vibrational bands are clearly visible for γ_0 and δ_0, as both parameters increase with the final vibrational level ν'. This behavior is expected, since γ_0 and δ_0 are proportional to the averaged values of the PBXS and PSXS which, in general, increase with the vibrational band. The difference between the PBXS for the two isotopologues, shown in Fig. 2, is directly manifested in differences between pressure broadening coefficients in Fig. 4. For the bands with lower ν', γ_0 in HD is dominated by the inelastic contribution at 296 K. Hence, γ_0 is much larger for HD than for H_2, for which the inelastic contribution is considerably reduced due to the lack of collision-induced transitions between para- and ortho-H_2 and larger rotational spacing. In the case of the S(0) 0-0 line, γ_0 for HD is more than ten times larger than for the H_2 molecule. As the ν' increases, the elastic contribution that comes mainly from the difference in radial coupling terms of the potential in the initial and final states becomes more important and γ_0 in H_2 becomes even slightly larger than in HD.

The dependences of γ_2 and δ_2 on the vibrational band mirror the dependences of γ_0 and δ_0 – they become larger as the speed-averaged pressure broadening and shift increase. The real and imaginary part of the Dicke coefficient $\tilde{\nu}_{opt}$, in turn, decrease with the vibrational band. Although the RDXS and the absolute value of IDXS grow with ν', the velocity-changing effect is correlated with coherence damping and dephasing and, as it can be seen in Eq. (6) for the Dicke parameter, σ_0^q cross-section is included in the equation.

The pressure broadening coefficient decreases with the initial rotational number j'' due to the fact that each subsequent rotational level differs increasingly in energy in accordance to the quadratic relation $E_{j''} = Bj''(j''+1)$. This behavior was also observed before in many collisional systems [50–52]. For purely rotational lines, γ_0 drops to nearly zero as j'' increases because the elastic contribution, emerging from the difference of initial and final molecular wavefunctions, is very low (for pure rotational lines, the vibrational state is the same and only a slight role is played by centrifugal distortion), and because the states with higher j'' are less sensitive to the elastic effects coming from the attractive part of a PES. In the case of H_2 molecule, γ_0 coefficient is very small thus the dependence on j'' is not well pronounced. For rovibrational bands in HD, γ_0 generally also decrease with j'', but as it can be seen in Ref. [19] for H_2 it is not always the case. As an example, for the Q branch of the 2-0 band, γ_0 is not monotonic at the beginning and for higher j'' it has a nearly constant value. Thus, it is another manifestation of the isotopologue dependence. Again, the δ_2 and γ_2 coefficients mirror the dependence of γ_0 and δ_0. Due to the relatively low value of γ_0 for purely rotational lines and nearly transition independent RDXS, the real part of Dicke parameter $\tilde{\nu}^r_{opt}$ is almost constant with j''. Comparisons of *ab initio* calculations with available experimental data can be found in Refs. [25,26]. There is a need for accurate measurements of the line-shape for rovibrational transitions for further validation.

To estimate the uncertainties of our *ab initio* results, we perform some additional calculations for the R(0) line of the 1-0 band at temperatures 77 K, 195 K, and 296 K, and investigate how the variation of the PES and dynamical numerical parameters of the propagation process (the initial and final points of the propagation, the propagation step and the number of asymptotically closed energy channels) affect the value of the *ab initio* coefficients. Conservative estimations show that the uncertainty of the used PES [1] is not greater than 1 % [21]. Thus, we repeat the calculation using potential radial terms multiplied by 1.01 and for the considered cases the highest obtained deviation is 0.45 %. The convergence of our calculations with the dynamical numerical parameters is obtained as follows. We set the initial and the final points of the propagation, R_{min} and R_{max}, the number of propagation steps, and the number of asymptotically closed energy channels such that only a sub-percent deviation of the line-shape parameters is introduced upon halving of R_{min} and R_{max}, doubling the number of propagation steps and adding the next asymptotically closed energy level. In total, we estimate the uncertainty of the calculated parameters at 0.6 %. It should be noted that in the case of interpolated and extrapolated parameters for the weaker transitions the deviation may be higher. There is also a second type of uncertainty originating from the DPL approximation (estimated by the root mean square error in the prioritized temperature range). The total combined uncertainty of each parameter is provided in the supplementary materials in the column DPL-err [28].

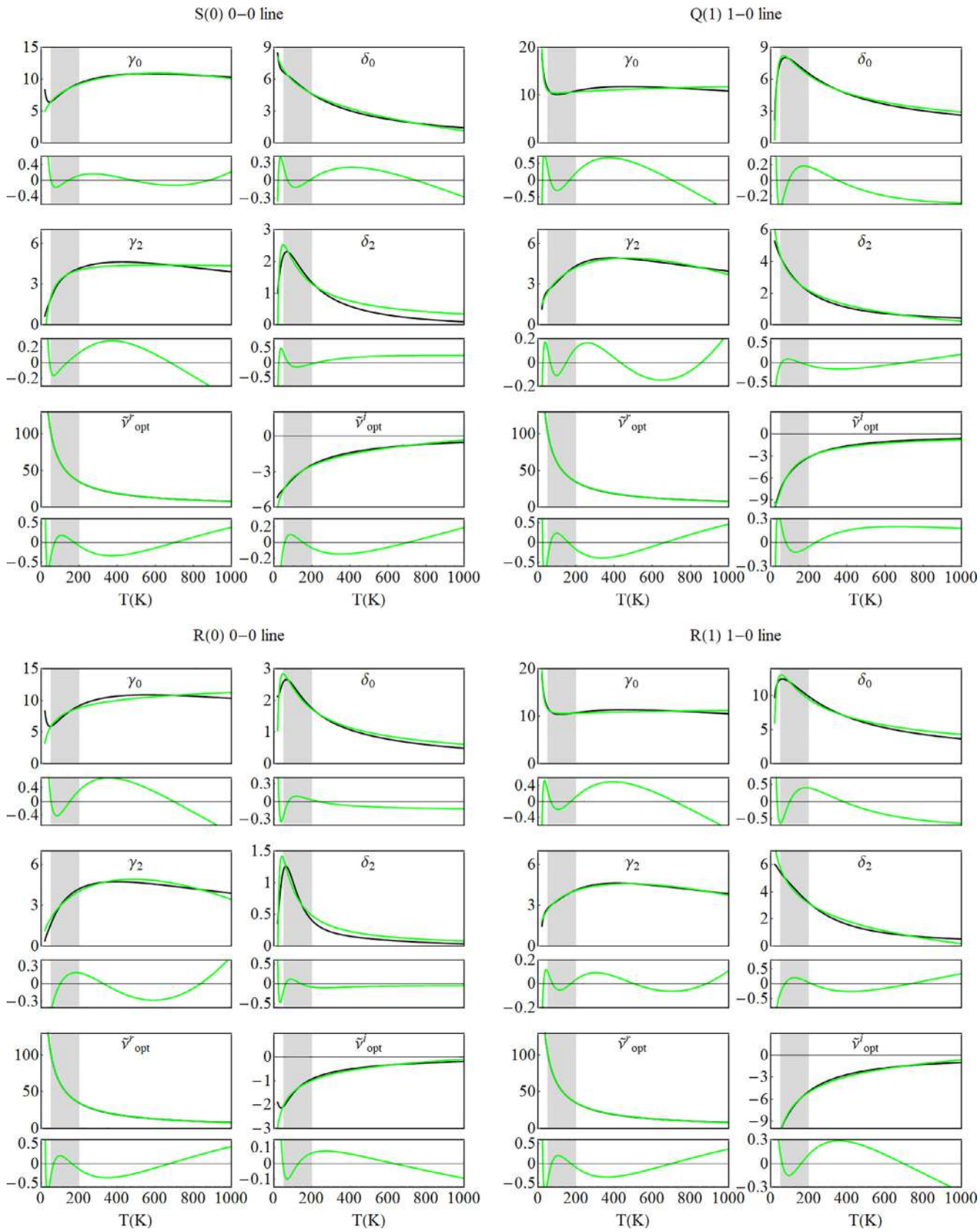

Fig. 3. Temperature dependences of the six collisional line-shape parameters, γ_0, δ_0, γ_2, δ_2, $\tilde{\nu}^{r}_{opt}$ and $\tilde{\nu}^{i}_{opt}$, for the four sample lines of HD perturbed by He. The black and green lines are the *ab initio* values and DPL representations, respectively. Each large graph is accompanied by a small one, presenting the residuals of the DPL fits. The vertical axes for all the panels (including residuals) are in 10^{-3}cm^{-1}atm^{-1}. The gray-shaded areas indicate the temperature range prioritized in the DPL fits. (For interpretation of the references to colour in this figure legend, the reader is referred to the web version of this article.)

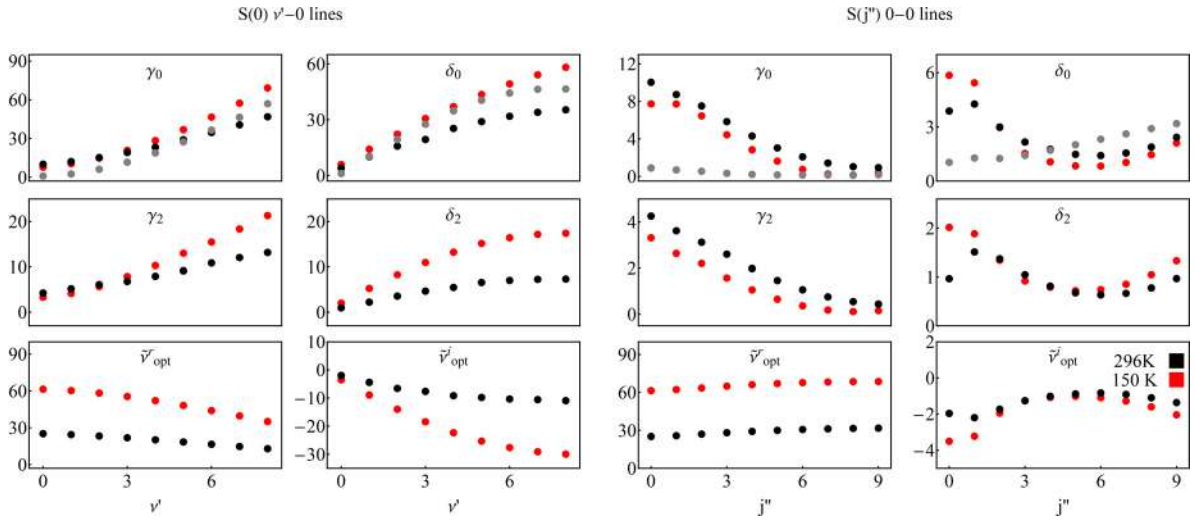

Fig. 4. Examples of the vibrational and rotational dependences of the six line-shape parameters reported in our dataset. Red and black dots correspond to the line-shape parameters for HD-He system at 150 K and 296 K, respectively. For comparison, we also added values of the line-shape parameters for the H_2-He system at $T = 296$ K marked by gray dots. All the parameters are expressed in units of 10^{-3} $cm^{-1}atm^{-1}$. The values of the line-shape parameters shown in this plot are not directly taken from *ab initio* calculations, but reconstructed from the DPL relations, Eqs. (7), based on the coefficients from our dataset.

4. Conclusion

Using the methodology presented in Ref. [19] to we performed accurate *ab initio* quantum scattering calculations, obtaining generalized spectroscopic cross-sections and line-shape parameters for electric dipole and quadrupole transitions within the ground electronic state for He-perturbed HD. The line-shape parameters describe the pressure broadening and shift, γ_0, δ_0, and the most important beyond-Voigt effects, the speed-dependences of γ_0, δ_0 through quadratic approximation, γ_2, δ_2, and the velocity-changing collisions through the complex Dicke parameter $\tilde{\nu}_{opt}$. Temperature dependences of the line-shape parameters were expressed by the double-power-law representation recommended for the HITRAN database. Calculations of generalized spectroscopic cross-sections were performed in kinetic energy range from 0.1 to 9000 cm^{-1} and line-shape parameters were obtained at temperatures from 20 to 1000 K which is the relevant range for investigations of gas giants and exoplanets atmospheres. The *ab initio* results cover all transitions including hot bands which involve vibrational levels from 0 to 5 or 8 and rotational levels from 0 to 6 and 9 to 11. Such a wide range was fully sufficient for populating all strongest and most important transitions and a great number of weaker ones. The values for exotic lines were obtained by interpolation and extrapolation of our *ab initio* results. This allowed us to populate all 11 575 rovibrational lines present in the HITRAN database. Comparison with values for H_2-He system led to the observation of strong isotopologue dependence for hydrogen molecule and helium atom system which arises mainly from the limitation of inelastic contribution in the case of H_2. Calculated generalized spectroscopic cross-sections, line-shape parameters, and double-power-law coefficients are provided in the supplementary material [28].

In principle, our methodology can be readily applied to any diatomic molecule in a $^1\Sigma$ electronic state interacting with a structureless atom. Similar calculations could also be done for not too massive linear molecules interacting with an atom, for example, C_2H_2-Ne [53]. For simple diatomic or linear molecules manifesting fine [54] or hyperfine structure [55], the theory (for recoupling the various angular momenta) exists and could be used to produce line-shape parameters for selected lines. Usually, the main problem which one needs to overcome during the calculations for more massive systems is the increased size of the basis caused by the fact that more massive molecules have lower rotational constants, and thus, their rotational levels are less energetically separated. Nevertheless, such calculations could be handled for selected lines of various rovibrational bands by neglecting the rovibrational couplings, i.e. the potential centrifugal distortion. One may also limit the calculations to the transitions that do not involve high vibrational bands.

For two interacting diatomic or linear molecules calculations become more challenging. However, numerous attempts have been already conducted within the above limitations for selected transitions. The examples of these are molecules in dihydrogen baths such as CO-H_2 [56], N_2 - H_2 [57] or C_2H_2 - H_2 [58,59]. Recently, successful attempts were performed for some collisional partners relevant from the perspective of Earth's atmosphere studies – Ar-perturbed CO [60], N_2-perturbed CO [61,62] and N_2-perturbed O_2 [63] (the last work is also an example of application of the method for an active molecule with non-zero spin).

The problem of a large rotational basis may be addressed through the use of various approximations such as the coupled state approximation [61] or its improved version that includes the nearest neighbor Coriolis coupling [64]. The efficiency of these approximations should be more deeply investigated in the future. For some systems, the limitation of the method may be imposed by the absence of sufficiently accurate potential energy surfaces including the vibrational dependence of the active molecule.

Declaration of Competing Interest

The authors declare that they have no known competing financial interests or personal relationships that could have appeared to influence the work reported in this paper.

CRediT authorship contribution statement

Kamil Stankiewicz: Conceptualization, Software, Investigation, Writing – original draft, Writing – review & editing, Visualization. **Nikodem Stolarczyk:** Conceptualization, Software, Investigation, Validation, Writing – original draft, Writing – review & editing, Visualization. **Hubert Jóźwiak:** Conceptualization, Software, Investigation, Validation, Writing – review & editing. **Franck Thibault:** Conceptualization, Methodology, Software, Resources, Writing – review & editing. **Piotr Wcisło:** Conceptualization, Methodology,

Writing – review & editing, Supervision, Project administration, Funding acquisition.

Acknowledgment

KS contribution is supported by the National Science Centre in Poland through project no. 2018/30/E/ST2/00864. HJ and PW contributions are supported by the National Science Centre in Poland through project no. 2018/31/B/ST2/00720. NS contribution is supported by the National Science Centre in Poland through project no. 2019/35/B/ST2/01118. The project is supported by the French-Polish PHC Polonium program (project 42769ZK for the French part). The project is co-financed by the Polish National Agency for Academic Exchange under the PHC Polonium program (dec.PPN/X/PS/318/2018). The research was part of the program of the National Laboratory FAMO in Toruń, Poland. Part of the calculations have been carried out using resources provided by Wroclaw Centre for Networking and Supercomputing (http://wcss.pl), grant no. 546.

Supplementary material

Supplementary material associated with this article can be found, in the online version, at doi:10.1016/j.jqsrt.2021.107911.

References

[1] Thibault F, Patkowski K, Zuchowski P, Jóźwiak H, Ciuryło R, Wcisło P. Rovibrational line-shape parameters for H_2 in he and new H_2-He potential energy surface. J Quant Spectrosc Radiat Transf 2017;202:308–20. doi:10.1016/j.jqsrt.2017.08.014.

[2] Bakr B, Smith D, Patkowski K. Highly accurate potential energy surface for the He-H_2 dimer. J Chem Phys 2013;139:144305. doi:10.1063/1.4824299.

[3] Czachorowski P, Puchalski M, Komasa J, Pachucki K. Nonadiabatic relativistic correction in H_2, D_2, and HD. Phys Rev A 2018;98:052506. doi:10.1103/PhysRevA.98.052506.

[4] Komasa J, Puchalski M, Czachorowski P, Lach G, Pachucki K. Rovibrational energy levels of the hydrogen molecule through nonadiabatic perturbation theory. Phys Rev A 2019;100:032519. doi:10.1103/PhysRevA.100.032519.

[5] Nolte J, Stancil P, Lee T, Balakrishnan N, Forrey R. Rovirational quenching rate coefficients of HD in collisions with He. Astrophys J 2012;744:62. doi:10.1088/0004-637x/744/1/62.

[6] Feuchtgruber H, Lellouch E, Orton G, Graauw T, Vandenbussche B, Swinyard B, et al. The D/H ratio in the atmospheres of Uranus and Neptune from Herschel-PACS observations. Astron Astrophys 2013;551:A126. doi:10.1051/0004-6361/201220857.

[7] Sung K, Wishnow E, Manceron L, Drouin B, Nixon C. Progress report on the measurements of pressure-broadening of HD rotational transitions for Jovian atmospheres. Bulletin of the AAS 2020;52.

[8] Lellouch E, Bézard B, Fouchet T, Feuchtgruber H, Encrenaz T, Graauw T. The deuterium abundance in Jupiter and Saturn from ISO-SWS observations. Astron Astrophys 2001;370:610–22. doi:10.1051/0004-6361:20010259.

[9] Miller-Ricci E, Sasselov D, Seager S. The atmospheric signatures of super-Earths: how to distinguish between hydrogen-rich and hydrogen-poor atmospheres. Astrophys J 2008;690:1056–67. doi:10.1088/0004-637X/690/2/1056.

[10] Dicke RH. The effect of collisions upon the Doppler width of spectral lines. Phys Rev 1953;89:472–3. doi:10.1103/PhysRev.89.472.

[11] Berman PR. Speed-dependent collisional width and shift parameters in spectral profiles. J Quant Spectrosc Radiat Transf 1972;12:1331–42. doi:10.1016/0022-4073(72)90189-6.

[12] Hess S. Kinetic theory of spectral line shapes. The transition between Doppler broadening and collisional broadening. Physica 1972;61:80–94. doi:10.1016/0031-8914(72)90035-3.

[13] Ciuryło R, Bielski A, Drummond JR, Lisak D, May AD, Pine AS, et al. High-resolution studies on the influence of velocity-changing collisions on atomic and molecular line shapes. AIP Conf Proc 2002;645:151–60. doi:10.1063/1.1525447.

[14] Tran H, Hartmann J-M, Chaussard F, Gupta M. An isolated line-shape model based on the Keilson-Storer function for velocity changes. II. molecular dynamics simulations and the Q(1) lines for pure H_2. J Chem Phys 2009;131:154303. doi:10.1063/1.3247898.

[15] Hartmann J-M, Tran H, Ngo NH, Landsheere X, Chelin P, Lu Y, et al. *Ab initio* calculations of the spectral shapes of CO_2 isolated lines including non-Voigt effects and comparisons with experiments. Phys Rev A 2013;87:013403. doi:10.1103/PhysRevA.87.013403.

[16] May A, Liu W-K, McCourt F, Ciuryło R, Sanchez-Fortún Stoker J, Shapiro D, et al. The impact theory of spectral line shapes: a paradigm shift. Can J Phys 2013;91:879–95. doi:10.1139/cjp-2012-0345.

[17] Tennyson J, Bernath P, Campargue A, Csaszar A, Daumont L, Gamache R, et al. Recommended isolated-line profile for representing high-resolution spectroscopic transitions (IUPAC Technical Report). Pure Appl Chem 2014;86:1931–43. doi:10.1515/pac-2014-0208.

[18] Fortney JJ, Robinson TD, Domagal-Goldman S, Genio ADD, Gordon IE, Gharib-Nezhad E, et al. The need for laboratory measurements and *ab initio* studies to aid understanding of exoplanetary atmospheres. arXivorg 2019.

[19] Wcisło P, Thibault F, Stolarczyk N, Jóźwiak H, Słowiński M, Gancewski M, et al. The first comprehensive dataset of beyond-Voigt line-shape parameters from *ab initio* quantum scattering calculations for the HITRAN database: He-perturbed H_2 case study. J Quant Spectrosc Radiat Transf 2021;260:107477. doi:10.1016/j.jqsrt.2020.107477.

[20] Thibault F, Wcisło P, Ciuryło R. A test of H_2-He potential energy surfaces. Eur Phys J D 2016;70:236. doi:10.1140/epjd/e2016-70114-9.

[21] Jóźwiak H, Thibault F, Stolarczyk N, Wcisło P. *Ab initio* line-shape calculations for the S and O branches of H_2 perturbed by He. J Quant Spectrosc Radiat Transf 2018;219:313–22. doi:10.1016/j.jqsrt.2018.08.023.

[22] Gordon IE, Rothman LS, Hargreaves RJ, Hashemi R, Karlovets EV, Skinner FM, et al. The HITRAN2020 molecular spectroscopic database. J Quant Spectrosc Radiat Transf (submitted) 2021.

[23] Słowiński M, Thibault F, Tan Y, Wang J, Liu A-W, Hu S-M, Kassi S, Campargue A, Konefał M, Jóźwiak H, Patkowski K, Zuchowski P, Ciuryło R, Lisak D, Wcisło P. H_2-He Collisions: *ab initio* theory meets cavity-enhanced spectra. Phys Rev A 2020:052705. doi:10.1103/PhysRevA.101.052705.

[24] Słowiński M, Jóźwiak H, Gancewski M, Stankiewicz K, Stolarczyk N, Tan Y, et al. Collisional line-shape effects in accurate He-perturbed H_2 spectra. J Quant Spectrosc Radiat Transf (submitted) 2021.

[25] Thibault F, Martínez R, Bermejo D, Wcisło P. Line-shape parameters for the first rotational lines of HD in He. Mol Astrophys 2020:100063. doi:10.1016/j.molap.2020.100063.

[26] Stankiewicz K, Jóźwiak H, Gancewski M, Stolarczyk N, Thibault F, Wcisło P. *Ab initio* calculations of collisional line-shape parameters and generalized spectroscopic cross-sections for rovibrational dipole lines in HD perturbed by He. J Quant Spectrosc Radiat Transf 2020;254:107194. doi:10.1016/j.jqsrt.2020.107194.

[27] Stolarczyk N, Thibault F, Cybulski H, Jóźwiak H, Kowzan G, Vispoel B, et al. Evaluation of different parameterizations of temperature dependences of the line-shape parameters based on *ab initio* calculations: Case study for the HITRAN database. J Quant Spectrosc Radiat Transfr 2020;240:106676. doi:10.1016/j.jqsrt.2019.106676.

[28] Stankiewicz K, Stolarczyk N, Jóźwiak H, Thibault F, Wcisło P. Supplementary material. J Quant Spectrosc Radiat Transf 2021.

[29] Wcisło P, Thibault F, Zaborowski M, Wójtewicz S, Cygan A, Kowzan G, et al. Accurate deuterium spectroscopy for fundamental studies. J Quant Spectrosc Radiat Transf 2018;213:41–51. doi:10.1016/j.jqsrt.2018.04.011.

[30] Pine A. Asymmetries and correlations in speed-dependent Dicke-narrowed line shapes of argon-broadened HF. J Quant Spectrosc Radiat Transf 1999;62:397–423. doi:10.1016/S0022-4073(98)00112-5.

[31] Rautian SG, Sobel'man II. The effect of collisions on the Doppler broadening of spectral lines. Sov Phys Uspekhi 1967;9:701–16. doi:10.1070/PU1967v009n05ABEH003212.

[32] Ciuryło R, Jaworski R, Jurkowski J, Pine AS, Szudy J. Spectral line shapes modeled by a quadratic speed-dependent Galatry profile. Phys Rev A 2001;63:032507. doi:10.1103/PhysRevA.63.032507.

[33] Rohart F, Mäder H, Nicolaisen H. Speed dependence of rotational relaxation induced by foreign gas collisions: studies on CH_3F by millimeter wave coherent transients. J Chem Phys 1994;101:6475–86. doi:10.1063/1.468342.

[34] Arthurs A, Dalgarno A. The theory of scattering by a rigid rotator. Proc R Soc A 1960;256:540–51. doi:10.1098/rspa.1960.0125.

[35] Flower D. Molecular collisions in the interstellar medium. Cambridge University Press; 2007. doi:101017/cbo9780511536229.

[36] Jóźwiak H., Gancewski M., Stankiewicz K., Wcisło P. BIGOS computer code. to be published

[37] Johnson BR. The renormalized Numerov method applied to calculating bound states of the coupled-channel Schrödinger equation. J Chem Phys 1978;69:4678–88. doi:10.1063/1.436421.

[38] Manolopoulos DE. An improved log derivative method for inelastic scattering. J Chem Phys 1986;85:6425–9. doi:10.1063/1.451472.

[39] Johnson B. Multichannel log-derivative method for scattering calculations. J Comput Phys 1973;13:445–9. doi:10.1016/0021-9991(73)90049-1.

[40] Monchick L, Hunter L. Diatomic-diatomic molecular collision integrals for pressure broadening and Dicke narrowing - A generalization of Hess's theory. J Chem Phys 1986;85:713–18. doi:10.1063/1.451277.

[41] Schaefer J, Monchick L. Line broadening of HD immersed in He and H_2 gas. Astron Astrophys 1992;265:859–68.

[42] Shafer R, Gordon RG. Quantum scattering theory of rotational relaxation and spectral line shapes in H_2-He gas mixtures. J Chem Phys 1973;58:5422–43. doi:10.1063/1.1679162.

[43] Ben-Reuven A. Symmetry considerations in pressure-broadening theory. Phys Rev 1966;141:34–40. doi:10.1103/PhysRev.141.34.

[44] Schaefer J, Monchick L. Line shape cross sections of HD immersed in He and H_2 gas. I. Pressure broadening cross sections. J Chem Phys 1987;87:171–81. doi:10.1063/1.453612.

[45] Corey GC, McCourt FR. Dicke narrowing and collisional broadening of spectral lines in dilute molecular gases. J Chem Phys 1984;81:2318–29. doi:10.1063/1.447930.

[46] Mehrotra S, Bestmann G, Dreizler H, Mäder H. A contribution to the investigation of T_2relaxation: rotational transitions of OCS and SO_2. Zeitschrift für Naturforschung A 1984;39:633–6. doi:10.1515/zna-1984-0707.
[47] Cazzoli G, Dore L. Lineshape measurements of rotational lines in the millimeter-wave region by second harmonic detection. J Mol Spectrosc 1990;141:49–58. doi:10.1016/0022-2852(90)90277-W.
[48] Puzzarini C, Dore L, Cazzoli G. A comparison of lineshape models in the analysis of modulated and natural rotational line profiles: application to the pressure broadening of OCS and CO. J Mol Spectrosc 2002;216:428–36. doi:10.1006/jmsp.2002.8663.
[49] Mantz A, Thibault F, Cacheiro J, Fernandez B, Pedersen T, Koch H, et al. Argon broadening of the ^{13}CO R(0) and R(7) transitions in the fundamental band at temperatures between 80 and 297K: comparison between experiment and theory. J Mol Spectrosc 2003;222:131–41. doi:10.1016/S0022-2852(03)00200-5.
[50] Predoi-Cross A, Luo C, Sinclair P, Drummond J, May A. Line broadening and the temperature exponent of the fundamental band in CO-N_2 mixtures. J Mol Spectrosc 1999;198:291–303. doi:10.1006/jmsp.1999.7940.
[51] Hartmann J-M, Boulet C. Line shape parameters for HF in a bath of argon as a test of classical path models. J Chem Phys 2000;113:9000–10. doi:10.1063/1.1319346.
[52] Boulet C, Flaud P-M, Hartmann J-M. Infrared line collisional parameters of HCl in argon, beyond the impact approximation: Measurements and classical path calculations. J Chem Phys 2004;120:11053–61. doi:10.1063/1.1714794.
[53] Thibault F, Cappelletti D, Pirani F, Blanquet G, Bartolomei M. Molecular-beam scattering and pressure broadening cross sections for the acetylene-neon system. Eur Phys J D 2007;44:337–44. doi:10.1140/epjd/e2007-00180-y.
[54] Grimminck DLAG, Spiering FR, Janssen LMC, van der Avoird A, van der Zande WJ, Groenenboom GC. A theoretical and experimental study of pressure broadening of the oxygen A-band by helium. J Chem Phys 2014;140:204314. doi:10.1063/1.4878666.
[55] Ronningen TJ, De Lucia FC. Helium induced pressure broadening and shifting of HCN hyperfine transitions between 1.3 and 20 K. J Chem Phys 2005;122:184319. doi:10.1063/1.1895905.
[56] Faure A, Wiesenfeld L, Drouin B, Tennyson J. Pressure broadening of water and carbon monoxide transitions by molecular hydrogen at high temperatures. J Quant Spectrosc Radiat Transf 2013;116:79–86. doi:10.1016/j.jqsrt.2012.09.015.
[57] Gómez L, Martínez RZ, Bermejo D, Thibault F, Joubert P, Bussery-Honvault B, et al. Q-Branch linewidths of N_2 perturbed by H_2: experiments and quantum calculations from an ab initio potential. J Chem Phys 2007;126:204302. doi:10.1063/1.2731789.
[58] Thibault F, Ivanov SV, Buzykin OG, Gomez L, Dhyne M, Joubert P, et al. Comparison of classical, semiclassical and quantum methods in hydrogen broadening of acetylene lines. J Quant Spectrosc Radiat Transf 2011;112:1429–37. doi:10.1016/j.jqsrt.2011.02.011.
[59] Thibault F, Martínez RZ, Bermejo D, Ivanov SV, Buzykin OG, Ma Q. An experimental and theoretical study of nitrogen-broadened acetylene lines. J Quant Spectrosc Radiat Transf 2014;142:17–24. doi:10.1016/j.jqsrt.2014.03.009.
[60] Serov E, Stolarczyk N, Makarov D, Vilkov I, Golubiatnikov G, Balashov A, et al. CO-Ar collisions: *ab initio* model matches experimental spectra at a sub percent level over a wide pressure range. J Quant Spectrosc Radiat Transf 2021;272:107807. doi:10.1016/j.jqsrt.2021.107807.
[61] Jóźwiak H, Thibault F, Cybulski H, Wcisło P. *Ab initio* investigation of the CO-N_2 quantum scattering: the collisional perturbation of the pure rotational R(0) line in CO. J Chem Phys 2021;154:054314. doi:10.1063/5.0040438.
[62] Paredes-Roibás D, Martínez RZ, Jóźwiak H, Thibault F. Collisional line broadening and mixing in the Raman spectrum of CO perturbed by N_2: experimental measurements and theoretical calculations. J Quant Spectrosc Radiat Transf 2021:107868. doi:10.1016/j.jqsrt.2021.107868.
[63] Gancewski M, Jóźwiak H, Quintas-Sánchez E, Dawes R, Thibault F, Wcisło P. Fully quantum calculations of O_2–N_2 scattering using a new potential energy surface: collisional perturbations of the oxygen 118 GHz fine structure line. J Chem Phys (submitted) 2021.
[64] Yang D, Hu X, Zhang DH, Xie D. An improved coupled-states approximation including the nearest neighbor Coriolis couplings for diatom-diatom inelastic collision. J Chem Phys 2018;148:084101. doi:10.1063/1.5010807.